Urban Climate 21 (2017) 154–172

Contents lists available at ScienceDirect

Urban Climate

journal homepage: http://www.elsevier.com/locate/uclim

Urban traffic and induced air quality modeling and simulation: Methodology and illustrative example

Jihen Landolsi [a], Ferid Rehimi [b,c,*], Adel Kalboussi [a]

[a] LEM laboratory, Faculty of Science, Monastir University, Environment Avenue, 5019 Monastir, Tunisia
[b] Taibah University, College of Engineering, Department of Civil Engineering, Prince Naif Ibn Abdulaziz, Tayba, PO Box: 344, 41411 Madinah, Saudi Arabia
[c] LESTE Laboratory, ENIM, Monastir University, 12, Ibn El Jazzar Avenue, 5019 Monastir, Tunisia

ARTICLE INFO

Article history:
Received 29 January 2017
Received in revised form 19 April 2017
Accepted 15 June 2017

Keywords:
Macroscopic traffic modeling
Vehicular fleet characterization
Simplified Copert
Gaussian plume model
Air pollution

ABSTRACT

Modeling vehicular pollution in urban areas is essential in decision-making for urban planning and sustainable transport policies. Indeed, guaranteeing a breathable air quality in the acceptable levels specified by the World Health Organization (WHO) reinforces the road towards a sustainable urban development.
In this work, we present the methodology and the different steps for the implementation of a sustainable transport decision tool permitting to perform a macroscopic simulation of road traffic using a first-order approach using the Cell Transmission Model (CTM) approach and a Dynamic Node Transmission Model (DNTM) approach for intersections; an estimation of the linear emission rates of the roads based on fleet statistics and the implementation of the simplified COPERT4 method; and finally the estimation of the near-instantaneous concentration of pollutants in urban areas. This tool is used to estimate the map of CO and NOx pollutants in the vicinity of a roundabout in the city of Sousse-Tunisia for the reference year 2015.

1. Introduction

Sustainable development is generally summarized as an economic, social and environmental development, that is managed in an integrated way through policies of governance. Those are supposed to ensure a

* Corresponding author at: Taibah University, College of Engineering, Department of Civil Engineering, Prince Naif Ibn Abdulaziz, Tayba, PO Box: 344, 41411 Madinah, Saudi Arabia.
E-mail address: Rehimi_f@yahoo.fr (F. Rehimi).

http://dx.doi.org/10.1016/j.uclim.2017.06.002
2212-0955/

Nomenclature

a_{lim}	Max-acceleration (m/s^2)
$B^{(k)}$	The kilometric percentage of the vehicles of the class k
$C, C(x,y,z,t)$	Pollution concentration (ppm)
D_i	Supply functions
$dC_j(x,y,z,t)$	Pollution concentration generated by a continuous point source (g/m^3)
$e_4{}^{(k)}$	Mean unit emission of the light vehicle of the class k (g/s)
$e_{i,j}(t)$	The origin destination from origin I to destination j (veh/h)
$f_i^{(k)}$	Multiplication factor from *Euro* 4 to *Euro i*
N	Number of vehicles at the node intersection
$Ncell$	Number of the traffic cells of a road
N_{ij}	Number of vehicles inside the node intersection coming from the link i and targeting the exit j
N_{in}, N_{out}	Number of Entering/exiting roads
N_j	Number of nodes present at the junction and having the link j
NP	Number of segments used in pollution estimation for a road.
O_j	Supply function of the road j for the intersection exiting traffic
p_{vl}, p_{pl}	Proportion of respectively light and heavy vehicles in the vehicular fleet
q	Flow rate (veh/h)
q_c	Capacity/maximum flow rate of a road (veh/h)
$Q_j(t)$	Linear emissivity (g/s/m)
q_i	Flow rate leaving the cell i (veh/h)
q_j	Flow rate exiting for the intersection to the link j (veh/h)
q_p	Partial flow
S_{i+1}	Supply function of the cell $(i+1)$ of the considered road (veh/h)
sign	Sign function
x,y,z	Cartesian coordinates (m)
$(O', \vec{i}_{loc}, \vec{j}_{loc}, \vec{k})$	Local coordinates
$(O, \vec{i}, \vec{j}, \vec{k})$	Global coordinates
t	Time in seconds (s)
$\overline{U}_w$	Mean wind velocity (m/s)
U	Instantaneous mean space velocity (km/h)
U_f	Free traffic velocity km/h

Acronyms

CFL	Courant-Friedrichs-Lewy
CO	Carbon monoxide
CTM	Cell transmission model
DNTM	Dynamic Node Transmission Model
ESDHS	European Sustainable Development and Health Series
FIFO	First in, First Out
LWR	Lighthill, Whitham and Richards
NO	Nitrogen monoxide
NO_2	Nitrogen dioxide
NOx	Nitrogen oxides
OD	Origin-Destination matrix
WHO	World Health Organization

Greek letters

$\alpha_i^{(k)}$	Percentage of petrol or diesel NAV in the fleet complying with the Euro i norm

β_i	The rate of supply allocated to the traffic entering from the road i
γ_{ij}	Turning rate coefficient
Δ	Total demand of the intersection node (veh/h)
Δt	Time step (s)
Δx	Space Step (m)
δl_j	Element of a road representing a point source (m)
ρ	Vehicular density (veh/km)
σ_y,σ_z	Atmospheric dispersion coefficients (m)
$\Omega(N)$	Supply function of the intersection (veh/h)
ω_i	Elementary supplies (veh/h)
φ_j	Partial demands
σ_y,σ_z	Atmospheric dispersion coefficients (m)

fine balance and an improvement of the quality of citizen's life through these three aspects according to the European Sustainable Development and Health Series (ESDHS, 1997). The abusive use of fossil resources in industry and transportation, creates a climate imbalance (Casper, 2010) and engenders significant diseases infrequent in a healthy environment (WHO, 2005). Sustainable development is generally synonymous of an economic development inside a socially equitable model which preserves the environment (ESDHS, 1997; Elliott, 2013).

Preserving the environment essentially means avoiding any form of pollution that can lead to a degradation of the ecosystem and the urban environment. This pollution can affect air, water and soil. In urban areas, the quality of the air we breathe conditions our health (Lipfert, 2016) and the health of future generations (Deng et al., 2016). For this purpose and in order to be in agreement with the limit levels defined by the WHO (2005), local authorities and cities are setting up stations for measurements of air quality in addition to some numerical tools for decision-making, permitting the estimation of the maps of the various pollutants in urban environment. These numerical tools may sometimes be the only means of quantifying pollution, given the absence of measurement stations or the unavailability of these data.

In several developing countries (WHO, 2016), the lack of experimental observations or data leads to the use of indirect approaches such as the numerical estimation of average pollution levels geographical maps. In order to create a pollution map, there is a need to quantify the contribution of domestic, industrial and transportation activities. In urban areas the main cause of pollution is undoubtedly road traffic (Hossein Shahbazi et al., 2016).

The estimation of atmospheric pollution maps caused by urban transport requires knowledge of road traffic during the peak periods and all along the day, the vehicular emission rates through a survey of the vehicular fleet composition and their relative emissions levels along with the weather data (wind speed, direction and atmospheric class) and an accurate method for the calculation of the atmospheric dispersion (Venkatram and Horst, 2006).

The road traffic data comes from experimental observations on certain points or arcs of the urban network. These experimental observations are to be used to create numerical simulations which are supposed to reproduce reliable road traffic over the whole Urban network creating traffic patterns that can be static or dynamic, microscopic or macroscopic (Barceló, 2010; Treiber and Kesting, 2013; and Daiheng, 2016).

In this work, the choice is made to adopt a macroscopic modeling and simulation since it is sufficient for pollution studies (Rehimi and Landolsi, 2013), and it is more efficient for an entire city modeling and simulation. The macroscopic model adopted is a Cell Transmission model CTM (Daganzo, 1994) with bounded acceleration (Leclercq, 2002) for the roads and the Dynamic Node Transmission Model (DNTM) for different intersections (Lebacque, 2005; Tampère et al., 2011). This means that our emphasis would be on intersections' storage and transmission characteristics (Lebacque, 2003) rather than their geometry.

The estimation of linear emission rates of roads is an exercise that requires an accurate knowledge of the fleet in terms of spectrum and emission levels. Several vehicular emission models are used in practice and they can be instantaneous, stochastic or physical models (Demir et al., 2014). The more applicable models

are Mobile 6 (EPA, 2003); COPERT (Kouridis et al., 2010); HBEFA (Hausberger et al., 2009); VT-MICRO (Ahn et al., 2002); Emit (Cappiello et al., 2002). In our case study, we use the COPERT4 (Kouridis et al., 2010; CETU, 2012) since it has the advantage of being robust and reliable (Demir et al., 2014).

Finally, in order to estimate the dispersion of pollutants, there are several approaches to Gaussian methods with continuous sources as Caline 4 (Benson, 1989), CALPUFF (2000) for puff methods, OSPM (Berkowicz, 2000) methods and the Gaussian Line Method (Venkatram and Horst, 2006). In the present work, we adopt the line Gaussian method since it is simple to understand, to implement, and to calibrate with experimental observations (Fallah-Shorshani et al., 2015). In addition, the new atmospheric dispersion coefficients calculated for an urban environment by (Connan et al., 2015) represent an improvement of the method. Finally, the coupled traffic simulation and atmospheric dispersion tool is used to reproduce the traffic flow at a roundabout in the city of Sousse in Tunisia for the reference year 2015. The traffic results are used with the vehicular fleet emission's rates informations to evaluate the pollution maps of carbon monoxide CO and the Nitrogen oxides NOx in the vicinity of the roundabout.

2. Macroscopic traffic modeling and simulation

The road traffic level in a network is the result of the balance between the supply and the demand of the transport (Ortúzar and Willumsen, 2011). The transport supply is indeed the set of geometric characteristics that form the road network and the set of operational characteristics and rules that manage the traffic flow. The road network consists of the geometry of the roads comprising the network and the different intersections. The roads can be single or multi-lane and the intersections may be signalized, unsignalized or roundabouts. These intersections guarantee the exchange of road traffic between neighboring roads. The operational characteristics of a network are essentially the traffic rules (lights, speed limits, single direction, etc.) and the constraints as roads and intersections capacities (Chevallier and Leclercq, 2007; HCM, TRB, 2010).

To solve the road traffic problem in a network numerically, we need to model first the behavior of the traffic on each road and intersection on the network, then, we simulate this on computer. The traffic problem may be represented in microscopic or macroscopic levels (Treiber and Kesting, 2013). Here, the adopted approaches are the first order cell transmission model for roads (CTM) (Daganzo, 1994); and a dynamic node transmission model (DNTM) for the intersections (Lebacque, 2003). Thus, the traffic is defined through the variables: flow rate q(veh/h), the vehicular density ρ(veh/m) and the mean space velocity U(m/s). In point of fact, these variables are interrelated in/by the following system of equations:

$$\begin{cases} \dfrac{\partial \rho}{\partial t} + \dfrac{\partial q}{\partial x} = 0 \\ q = \rho.U \\ q = q_e(\rho) \end{cases} \tag{1}$$

where the equation q_e is the equilibrium flow rate given by the fundamental diagram equation.

2.1. Cell transmission model (CTM)

The cell transmission model is a numerical approach similar to finite volume techniques in fluid mechanic which was first introduced by Daganzo (1994). The method has seen many evolutions to many variants such as IT-CTM (Du and Dao, 2015 and Du et al., 2016). In the CTM method, the road is discretized into N_{cell} cells. These cells communicate with their neighbors by transmitting during an integration time step Δta certain number of cars. Every cell at the position x, at the time t transmit to its following neighbor a number of cars is equal to $q(x,t)\Delta t$. The flow rate $q(x,t)$ is obtained for each cell by using the numerical scheme of Godunov (Godunov, 1959) which is suitable for hyperbolic problems. During this step, we assume that the traffic variables are homogenous for each cell. The system (1) is discretized basing on the Lighthill, Whitham and Richards (1962) approach known as (LWR) approach with bounded acceleration (Leclercq, 2002, Treiber and Kesting, 2013).

The continuity equation is then written in discrete form as:

$$\rho_i(t+\Delta t)/\Delta t = \rho_i(t)/\Delta t - [q_i(t) - q_{i-1}(t)]/\Delta x \tag{2}$$

where $\rho_i(t)$ and $q_i(t)$ are respectively the mean density at the cell i at the time t and $q_i(t)$ is the mean flow rate leaving the cell i in the time range $(t, t+\Delta t)$.

We notice here that for an explicit numerical scheme, the Courant-Friedrichs-Lewy (CFL) condition $\frac{\Delta x}{\Delta t} \geq U_f$ has to be respected to avoid any divergence where U_f is the free velocity of the traffic.

The flow rate $q_i(t)$ depends on the adequation between demand ($D_i(t)$) of the cell i and the supply of the cell $i+1$ ($S_{i+1}(t)$) at the time interval $(t, t+\Delta t)$. This leads to:

$$q_i(t) = \min\left(S_{i+1}(t), D_i(x,t)\right) \tag{3}$$

and

$$S(\rho) = \frac{q_c}{2}(1 - sign(\rho - \rho_{cr})) + \frac{q_e(\rho)}{2}(1 + sign(\rho - \rho_{cr})) \tag{4}$$

$$D(\rho) = \frac{q_c}{2}(1 + sign(\rho - \rho_{cr})) + \frac{q_e(\rho)}{2}(1 - sign(\rho - \rho_{cr})) \tag{5}$$

where q_c (veh/h) is the capacity/maximum flow rate of the road and $\rho_{cr}(veh/km)$ is the critical vehicular density for which q_c is reached.

By adding the fact that the acceleration of the traffic flow in any cell is physically bounded by a limit value a_{lim}, the flow rate at the cell i at the time t is calculated as:

$$q_i(t) = Min\left(S_{i+1}(t),\ D_i(t),\ \rho_i(t)\left(U_i(t-\Delta t)\ \left(1 - \frac{\Delta t}{\Delta x}\ (U_i(t-\Delta t) - U_{i-1}(t-\Delta t))\right) + a_{\lim}\ \Delta t\right)\right) \tag{6}$$

When considering one single road, the Eq. (6) are considered and when we are studying a whole network with many origins and destinations, the Eq. (6) are still correct and we add to them the partial equation relative to every route path on the network. It is worth noting, that for the case of a network, we have many trips, starting from different origins i of the network to different destinations j with their correspondent flow rates functions $e(i,j)$ (t). In this case, the Eq. (6) are applied for each partial flow $qp(i,j)(t)$.

2.2. Dynamic node transmission model (DNTM)

We consider an urban intersection represented by a set of entering roads $i \in \langle 1, N_{in} \rangle$ and exiting roads $j \in \langle 1, N_{out} \rangle$. These roads are connected by an intersection node modeled as a point with an internal state and with a neglected physical dimension of the intersection, and a neglected vehicular dynamic inside it (Lebacque, 2003). This model is called dynamic node transmission model (DNTM). If $N_j(t)$ is the total number of vehicles present at the junction and having the link j as a destination, and $N(t)$ is the total number of vehicles at the node:

$$N = \sum_{j=1}^{N_{out}} N_j \tag{7}$$

The dynamic node intersection is characterized by an internal state $N(t)$, a demand function $\Delta(N)$ to the links downstream and a supply functions $\Omega(N)$ for the links upstream the node. The node can store a limit of $N = N_{max}$ vehicles.

The total supply of the node $\Omega(N)$ is spread into N_{in} elementary supplies ω_i as:

$$\omega_i = \beta_i \cdot \Omega(N), \tag{8}$$

With $\beta_i \forall i \epsilon \ \langle 1, N_{in} \rangle$, the rate of supply allocated to the traffic entering from the road i (Lebacque and Khoshyaran, 2005).

The partial demands associated to the downstream links are based on (First in, First Out) FIFO approach which permits to write:

$$\varphi_j = \frac{N_j}{N} \cdot \Delta(N(t)) \tag{9}$$

with $\forall i \epsilon \ \langle 1, N_{out.} \rangle$

Then, the flow rate $qin_i(t)$ entering to the node from the upstream link i is given by:

$$qin_i(t) = \ min(D_{Ncell}(i), \omega_i) \tag{10}$$

where $D_{Ncell}(i)$ is the demand the cell $Ncell$ of the road i at the entry of the intersection node.

The exiting traffic $qout_j(t)$ from the DNTM to the link j is given by:

$$qout_j(t) = \ min\left(\varphi_j, S_1(j)\right) \tag{11}$$

Where $S_1(j)$ is the traffic supply of the first cell of the road j to the intersection node.

The conservation of the cars entering/exiting the DNTM is written in dynamic form as:

$$\frac{dN}{dt} = \sum_{i=1}^{n} q_i(t) - \sum_{j=1}^{m} q'_j(t) \tag{12}$$

Finally:

$$\frac{dN_{ij}}{dt} = \gamma_{ij} q_i - \frac{N_{ij}}{N_j} q'_j \forall i, i = 1, \ldots, N_{in}, \forall j, j = 1, \ldots, N_{out} \tag{13}$$

with: γ_{ij} is the turning rate coefficient of the vehicles outgoing from the link i to the link j and can be static or dynamic.

3. Network pollution emission rates

3.1. Source emission models

The quantification of the vehicular emissions is delicate in practice, and it requires the knowledge of a number of parameters related to the vehicle such as vehicle age, maintenance, mileage, infrastructure, and others related to the weather and traffic conditions, Etc. For this reason, there are several models and approaches for estimating the pollution emitted at the source by the vehicular fleet.

The COPERT4 model is considered as one of the best models to date (Demir et al., 2014). It is based on the HBEFA (Hausberger et al., 2009) model and is more suitable for European or North African fleets that are similar. What is more, the COPERT4 model presents the properties of being more robust and reliable in the estimations than the other models (Demir et al., 2014). Thus, the COPERT4 model a used in the present work.

3.2. Pollution evaluation at the source: COPERT4 model

The COPERT4 model is an empirical model introduced by Kouridis et al. (2010) permitting to estimate mean emissions of a vehicular fleet. The evaluated emissions by this model are not instantaneous, but averaged over a fleet (Demir et al., 2014). The instantaneous behaviors related to the vehicles acceleration and deceleration, dynamics and the traffic state are implicitly included in the model and do not appear directly in the equations used in the calculations (Demir et al., 2014). The regression equations used in the calculations of the COPERT4 model appear to be long in implementation. Accordingly, we propose

to use a simplified methodology of the COPERT4 model proposed in CETU (2012). In this simplified COPERT4 model, vehicles are divided into two classes, which are gasoline and diesel. Gasoline vehicles are themselves subdivided into three subclasses according to cylinder size of the vehicle, while diesel engines are subdivided into two subclasses. It should also be noted that commercial cars are classified as diesel vehicles, and this simplification comes from statistical observations of the commercial cars (CETU, 2012).

The vehicular emission rates of pollutants are quantified relatively to the emissivity $e_4$of the Euro4 standard of the category studied for given conditions of speed and slope of the road. The pollution emission rate of a light petrol or diesel car in a car fleet is given by:

$$e_{VL} = \sum_{k\in Gas+Dis} p^{(k)} \left({e_4}^{(k)} \sum_{i=0}^{6} {\alpha_i}^{(k)} {f_i}^{(k)} \right) \tag{14}$$

With ${e_4}^{(k)}$: Mean unit emission of the light vehicle of the class k∈ {Gasoline, Diesel} for a given year and given conditions (velocity and slope of the road), $B^{(k)}$is the kilometric percentage of the vehicles of the class k, ${\alpha_i}^{(k)}$: Percentage of petrol or diesel NAV in the fleet complying with the *Euro i* norm for the year in question. The value for $i=0$ denotes vehicles complying with the pre-euro standard 1 (pre-euro) and ${f_i}^{(k)}$: multiplication factor from Euro 4 to *Euro i*(CETU, 2012).

Finally, the linear emissivity of a section of road is defined by:

$$E_l = p_{vl} e_{vl} + p_{PL} e_{PL} \tag{15}$$

4. Pollution dispersion: Line Gaussian dispersion model

The pollution concentration $dC_j(x,y,z,t)$ generated by a continuous point source having a length of δl_j and a linear emissivity $Q_j(t)$ under the effect of a mean wind of modulus

$\overline{U}_w$ in a space position $M(x,y,z)$ is given by the following equation:

$$C_j(t,x,y,z) = \frac{Q_j(t)\delta l_j}{2\pi \overline{U}_w \sigma_y \sigma_z} \; exp\left(\left(-\frac{y^2}{2\sigma_y^2} \right) + \left(-\frac{(z-h)^2}{2\sigma_z^2} \right) + \left(-\frac{(z+h)^2}{2\sigma_z^2} \right) \right) \tag{16}$$

where σ_y,$\sigma_z$are calculated according to the relations given by Pasquill and Smith (1983) and Connan et al. (2015), and according to corresponding the atmospheric stability class; and where the x-coordinate is in the wind direction, the y-coordinate is obtained by a 90° trigonometric rotation and z-coordinate is the altitude of the point.

The total pollution concentration $C(x,y,z,t)$ generated by a road [AB] at any point of space at time t is given by the Eq. (17) which is the result of an analytical integration of the Eq. (10) for inclined winds $\theta\in[-80,80]$:

$$\begin{aligned} C(x,y,z,t)_{[A,B]} = {} & \frac{Q(t)}{2\sqrt{2\overline{U}_w}\sigma_z\left(d_{eff}\right)} \; exp\left(\left(-\frac{(z-h)^2}{2\sigma_z\left(d_{eff}\right)^2} \right) + \left(-\frac{(z+h)^2}{2\sigma_z\left(d_{eff}\right)^2} \right) \right) \\ & \times \; erf\left(\frac{y\cos(\theta) - x\sin(\theta)}{\sqrt{2}\sigma_y(d_1)} \right) - erf\left(\frac{(y-L)\cos(\theta) - x\sin(\theta)}{\sqrt{2}\sigma_y(d_2)} \right) \end{aligned} \tag{17}$$

where $d_{eff} = {}^{x}/_{\cos(\theta)}$; $d_i = (x-x_i)\cos(\theta) + (y-y_i)\sin(\theta)$.

4.1. Pollution estimation in local and global coordinates

In practice, we have a network of roads; and the wind direction angle with each road of the network is not the same and varies from one day to another. In that, the first step of the computation consists of expressing the velocity vector of the wind in a local coordinate system in which the Eq. (17) can be used directly. This local coordinate system is constructed for each segment of the road (sometimes the road is curved and we

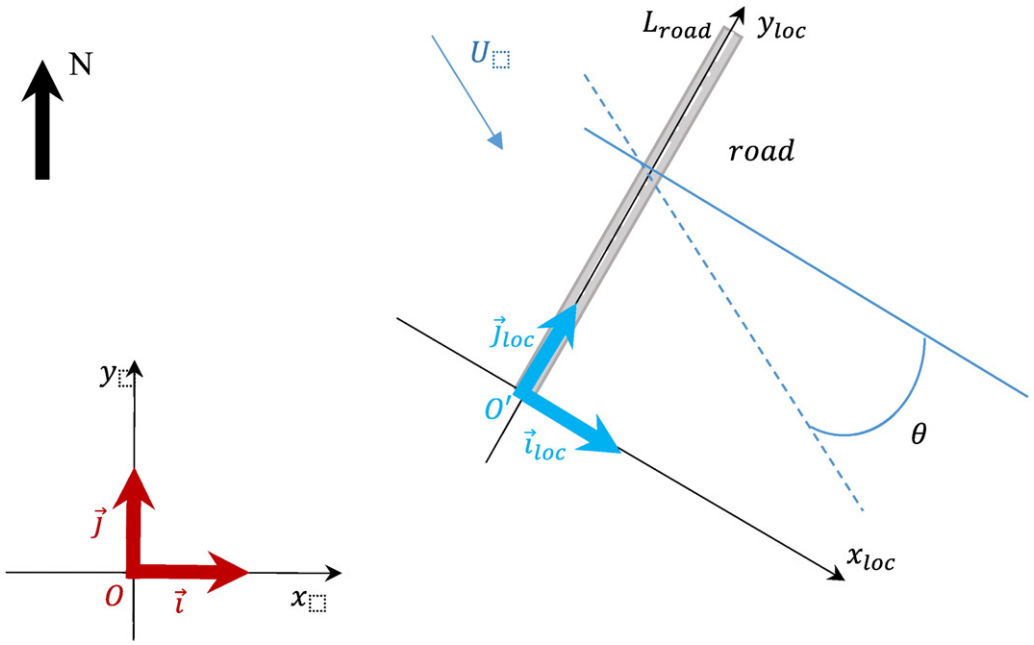

Fig. 1. Conversion from local to global coordinates.

need to construct these local coordinate systems for each segment) by taking the road as the ordinate axis. The *x*-axis is taken perpendicularly to the road and points in the same direction of the wind. The *z*-axis is oriented upwards and remains identical to the overall axis (Fig. 1). So, the calculation of the generated pollution by each road segment is calculated in a local coordinates system $(O', \vec{i}_{loc}, \vec{j}_{loc}, \vec{k})$ and converted after in the global coordinates system $(O, \vec{i}, \vec{j}, \vec{k})$ (Fig. 1).

Note also that for $\theta \in [80,90]$, the road or the element of road in which the calculations are done, is discretized into *NP* punctual portions of elementary lengths δl_j and the concentration of these points are summed to obtain accurate results and to guarantee the correctness of the calculations.

4.2. Case of a road network: calculation methodology

The case of a road network is a generalization of the case of a road. The concentration of the network emissions at any point in the urban environment is the sum of that generated by the entire urban network route. In this case, we write that:

$$C(x,y,z,t) = \sum_{road(i)} C(x,y,z,t)_{[road(i)]} \tag{18}$$

where $C(x,y,z,t)_{[road(i)]}$ is the contribution of the road *i* in the concentration $C(x,y,z,t)$.

5. Illustrative example: pollution levels estimation at a roundabout in Sousse city

5.1. Experiment procedure and traffic measurements

In order to estimate the pollution maps of some gases in the vicinity of a study called 20 March roundabout near the hospital of Sahloul in Sousse city (Fig. 2), we need to know the traffic, the vehicular fleet emission rates and the time resolved information about mean wind velocity. For such purpose, we carried out an estimation of the vehicle fleet on the basis of a survey on a number of vehicles related to Sousse city. This permits to quantify the vehicular emission rates according to the simplified COPERT4 method (CETU, 2012). Then,

Fig. 2. "Twenty March" roundabout, Sousse-City, Tunisia (Google Earth®).

these obtained emission rates are used with the road traffic results in order to quantify the instantaneous linear emission rates of the roads forming this intersection. The weather information, especially the instantaneous wind speed and direction during the simulation period, allows an almost instantaneous evaluation of the pollution maps of the different studied gases in the vicinity of the roundabout and also grants to estimate the different average maps of the studied pollutants. We notice here that the buildings in the vicinity of the studied intersection are generally ground plus one or two levels except two buildings (Fig. 2). This gives an average height of buildings about $H \approx 9$ m. As the width of the (roadway + sidewalk) is of the order of $W \approx 20$ m, we have an almost ratio $\frac{H}{W} \sim 0.45$–0.5. In this case, the use of a Gaussian plume model is justified (Soulhac et al., 2011).

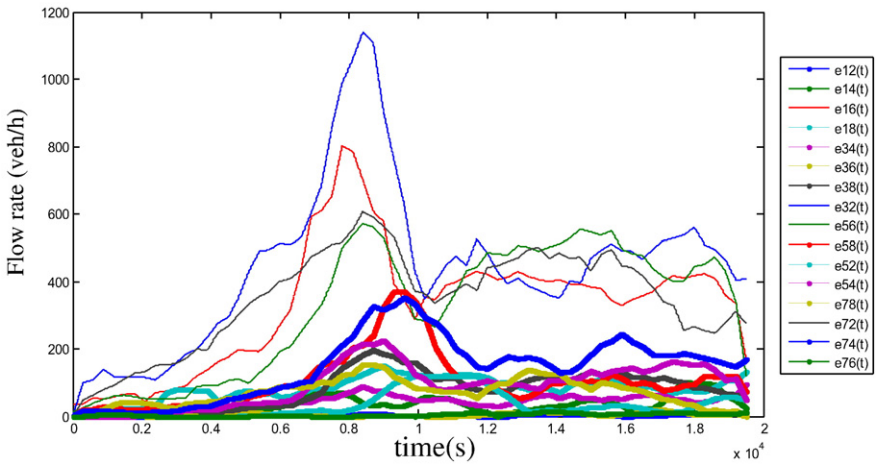

Fig. 3. Time evolution of the different 16 partial flow rates $e_{i,j}(t)$ at the entries of the roundabout.

The roads connected to the roundabout (Fig. 2) are characterized by a mean length for each leg of $L=$ 350 m with two lanes in each entry/exit. The fundamental diagram is taken as a triangular fundamental diagram, with a free speed: $U_f=40$ km/h Critical $\rho_{cr}=90$ veh/km and a saturation density: $\rho_j=350$ veh/km, $q_c=3600$ veh/h). The exchange zone is characterized by 08 inputs and 08 outputs (Fig. 2). Note also that the average length of a vehicle is about 04 m.

The traffic observations are carried out for a period of 5 h and 30 min on a typical day from 05:30 am to 11:00 am. The traffic is characterized by a morning peak hour around 07:50 am to 8:30 am and the traffic becomes almost constant after 08:30 am The traffic flows $e_{ij}(t)$ at the entries of the roads of this roundabout are presented in the following figure (Fig. 3) and where i is the origin leg and j is the destination leg.

5.2. Traffic simulation results

There are 16 possible routes, and every route is associated with a specific traffic demand $e_{i,j}(t)$ from an origin leg i to a destination j (Fig. 3). In this simulation, the traffic is decomposed according to the number of routes present in the simulation. For that, we decompose the flow into 16 partial flow streams. This aims at tracking the behavior of each flow from its origin until its arrival at the different destinations and hence guaranteeing a mass balance conservation of the vehicles in the network. In general, we define as many partial flows as practical routes in the network. In practice, a traveler takes maximum from three to five possible paths to go from an origin to a destination which means that the number of the routes or partial flows in a network is at maximum less than five times the number of origin-destination pairs.

The simulation of road traffic in this case study involves injecting demands $e_{ij}(t)$ at roads entries and solving the problem of the CTM and the DNTM for each of the different partial flows. Every road link is divided into $(N=40)$ cells of $\Delta x=13\ m$ length and the time step $\Delta t$is taken $\Delta t=1s$; $\Delta x=L/N$.

Since the origin-destination matrix is defined as $e_{ij}(t)$, the traffic demand that should pass across an entry road i is $e_{i\cdot}\ (=\sum_{j\in\{2,4,6,8\}} e_{ij})$, and that cross an exit road j is $e_{*j}\ (=\sum_{i\in\{1,3,5,7\}} e_{i,j})$.

The Fig. 4 represent a comparison between the simulated dimensionless traffic $q(t)/q_c$ simulated at the cell 20 of each road of the intersection with the dimensionless traffic demand that should cross this road which is $e_{i\cdot}/q_c$ for any entry road i and e_{*j}/q_c for any entry road j.

As long as the traffic is fluid and there is no congestion on the roads or any saturation (overload) at the intersection, there would be no big difference between the demand $e_{i\cdot}/q_c$ being injected at the entry of the road i and the simulated one $q(t)/q_c$ at the cell 20 of the road i. The only difference is the time shift taken by the traffic to reach the cell 20 from the entry. This may also apply to the simulated flow at any exit road j when comparing it with the injected flows e_{*j}/q_c. At the peak hour (from 07 h: 30 am to 08 h: 30 am), the traffic becomes dense, especially, at the intersection node, hence, we observe a difference between injected flows and the simulated ones at the nodes 20. This phenomenon is observed at the exit roads (2, 4, 6 and 8) at the peak hour, and appears when the dynamics and the interaction of the partial traffic flows (which are conflictual) becomes important and may create queues.

5.3. Source emission rate evaluation

5.3.1. Vehicular fleet composition

The vehicular fleet composition in Sousse city is estimated as part of a survey for the year 2015 at the technical cars control center in Sousse on a sample of 1000 randomly selected vehicles. Note that this fleet consists of 62.2% of gasoline-powered vehicles, 36.6% of vehicles running on diesel and 0.9% LPG. It should also be noted that 85% of the vehicles are with 4 cylinders, 9% with 3 cylinders and 6% for those more than 4 cylinders. The obtained results (Table 1) are close to the estimations of the French fleet (CETU, 2012). It is noteworthy too, that the characteristics of the French and Tunisian fleets are similar in terms of cylinder capacity and emissivity as Tunisian cars are predominantly French, German or Italian.

5.3.2. Emission rates evaluation of CO and NOx using Copert method

The simplified COPERT4 approach presented in Section 3.2 and proposed in CETU (2012) provides an estimation of the CO and NOx emissivity of a mean light vehicle running in the city of Sousse despite the

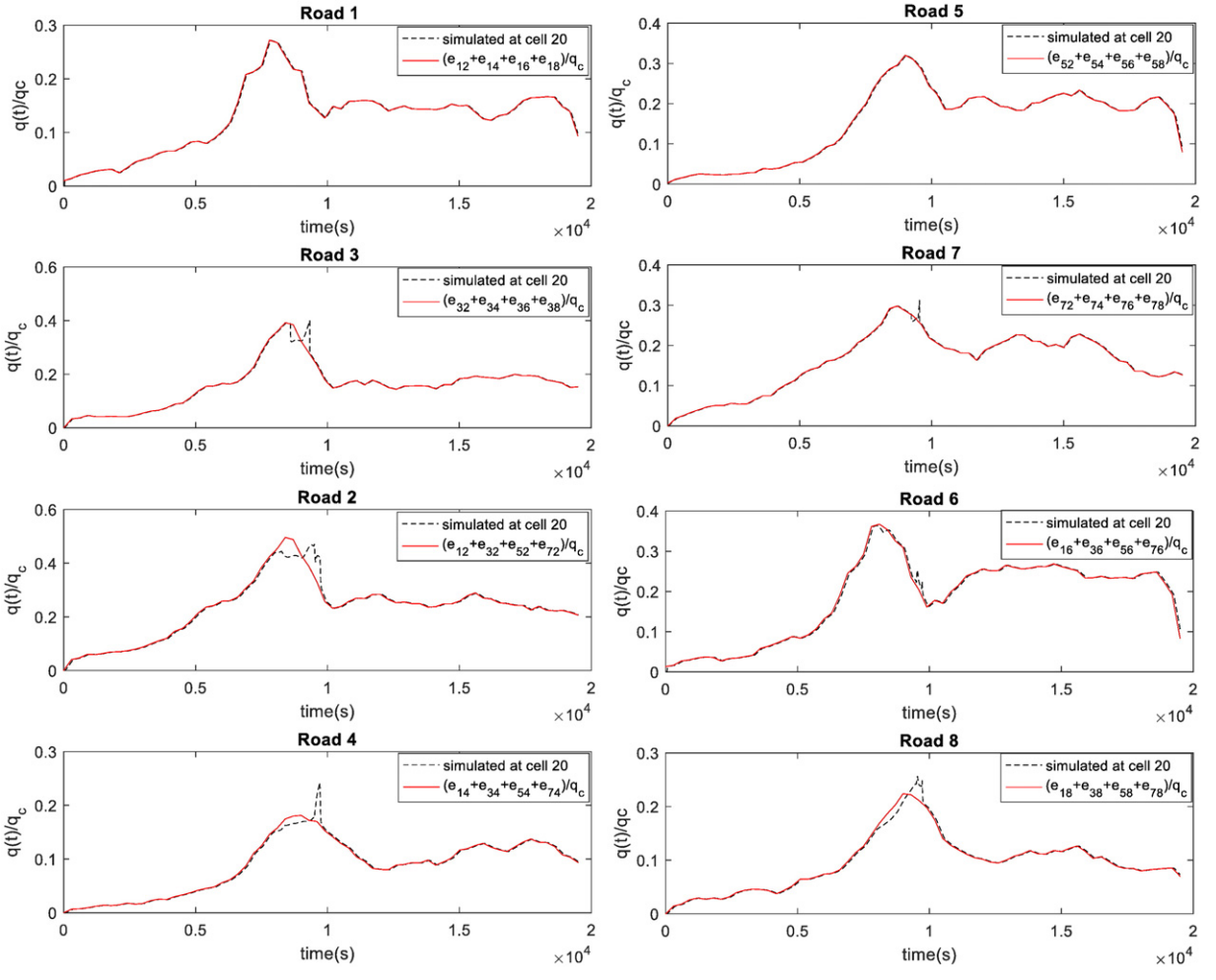

Fig. 4. Traffic demands passing through the roads versus simulated traffic at the cell 20 of each road.

Table 1
Vehicular fleet composition according to their kilometric travel distances in Sousse city in comparison with the French vehicular fleet for the reference year 2015.

	Diesel		Essence	
	Sousse	France	Sousse	France
Pre-Euro	3%	0.2%	3%	3%
Euro 1	3%	0.7%	3%	3%
Euro 2	7%	2.4%	7%	7%
Euro 3	20%	12.9%	17%	17%
Euro 4	34%	34%	37%	37%
Euro 5	33%	49.7%	33%	33%
Euro 6	–	–	–	–

fact that it is a Gasoline or Diesel vehicle. The results of the calculations are presented in the following figure (Fig. 5).

5.4. Meteorological data

The pollutants generated by the traffic are dispersed in the urban environment due to the wind. Henceforth, the meteorological information of the study period is essential for the quantification of the different pollutants concentrations. The figure (Fig. 6a) shows how the wind rises near the roundabout at a height of 02 m from the ground. The instantaneous information of the wind speed and angle are shown in the figure (Fig. 6b). The atmospheric stability class in the study was found to be of type "B" according to the Pasquill and Smith (1983) classification. The dispersion coefficients σ_y and σ_z are calculated according to the Connan et al. (2015) correlations for urban areas as follow:

$$\begin{cases} \sigma_y = 0.26\,x\,(1+0.001\,x)^{-1} \\ \sigma_z = 0.14\,x\,(1+0.0006\,x)^{-0.5} \end{cases} \tag{19}$$

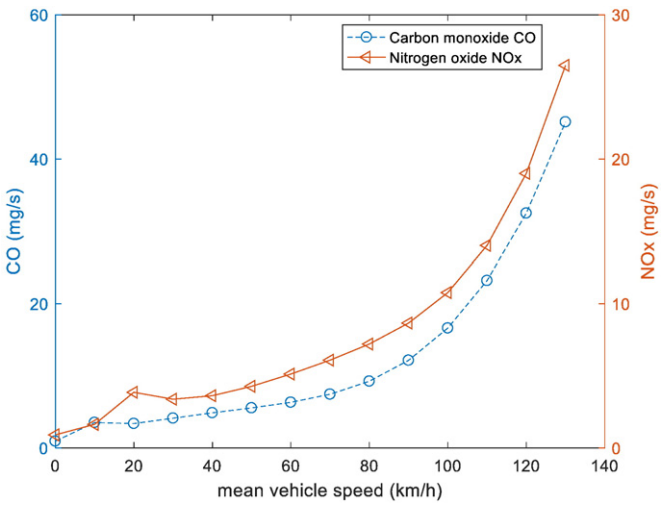

Fig. 5. Emission rate of a mean vehicle velocity in Sousse city for a road slope of 0% in 2015.

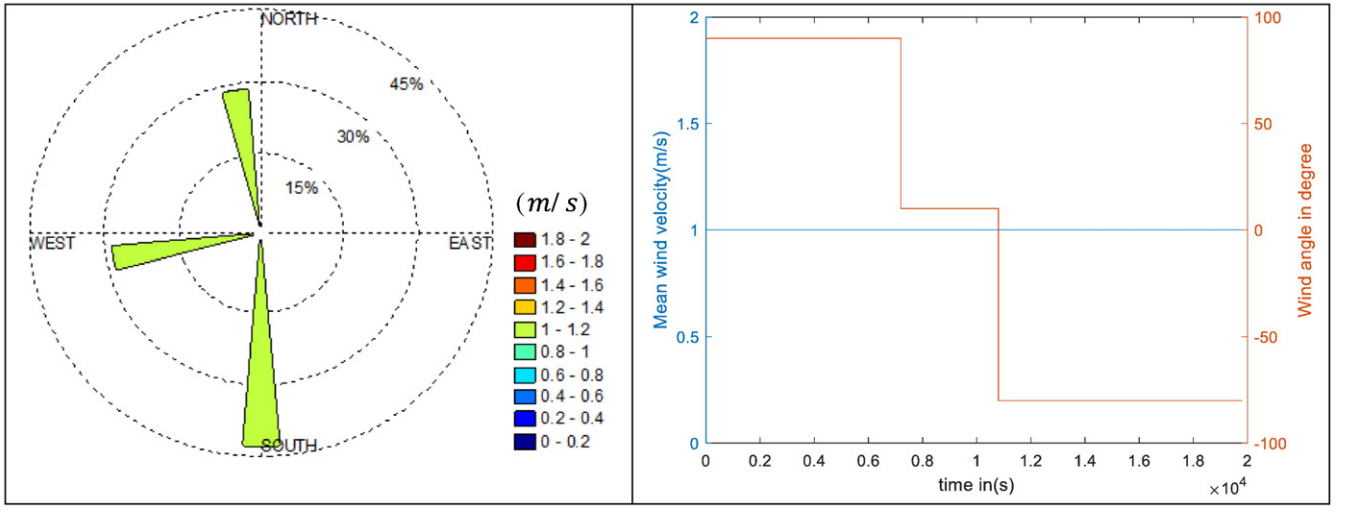

Fig. 6. (Left figure) Wind rose at 02 m near the roundabout; (right figure) Instantaneous mean wind velocity and wind angle.

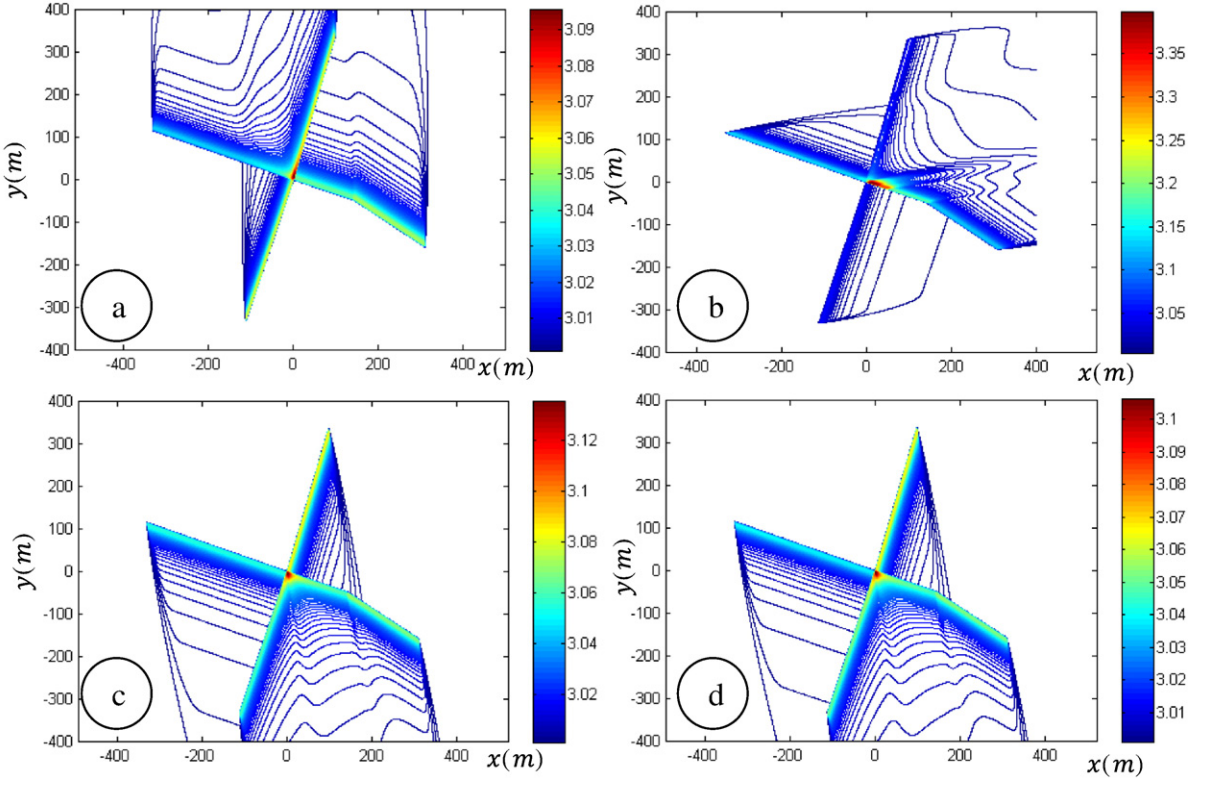

Fig. 7. Instantaneous CO (in ppm) concentration maps; a) $t = 6000$ s; b) $t = 8400$ s; c) $t = 15{,}600$ s; d) $t = 19{,}200$ s; at $z = 2$ m from the ground.

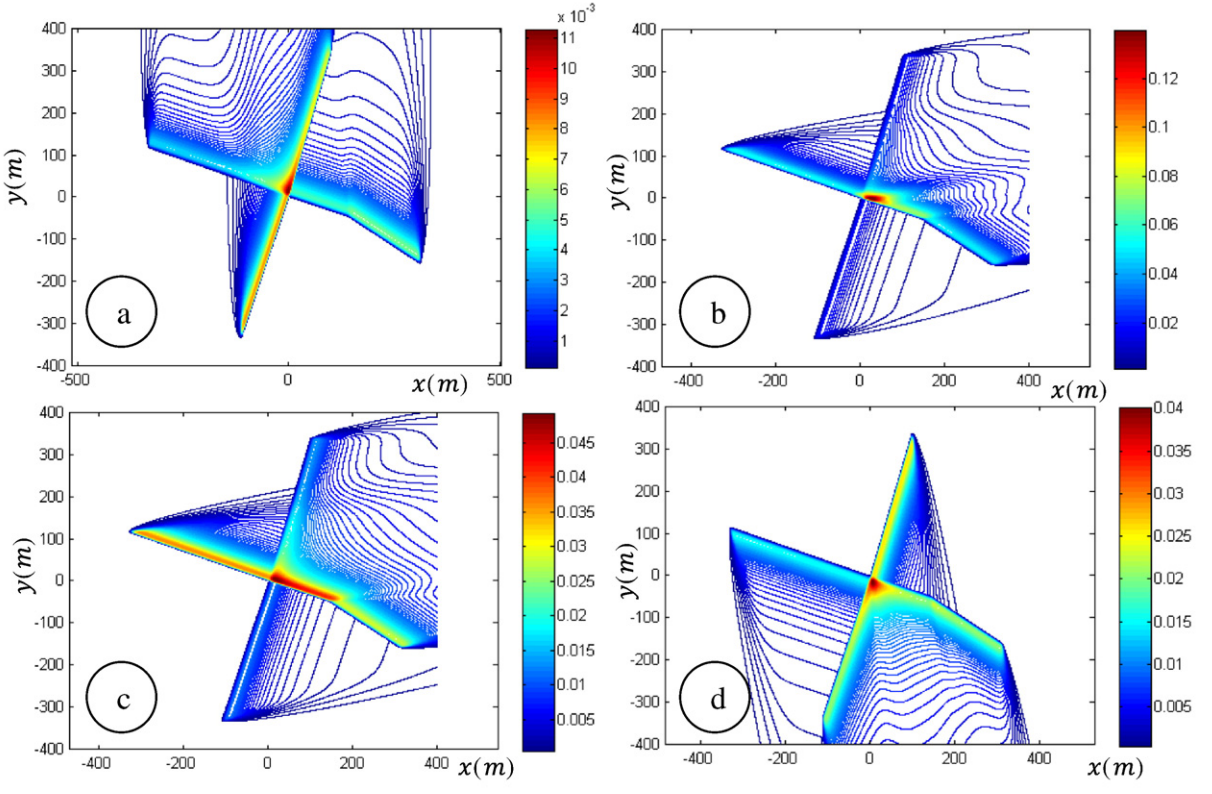

Fig. 8. Instantaneous NOx (in ppm) concentration maps; a) $t = 6000$ s; b) $t = 8400$ s; c) $t = 15{,}600$ s; d) $t = 19{,}200$ s; at $z = 2$ m from the ground.

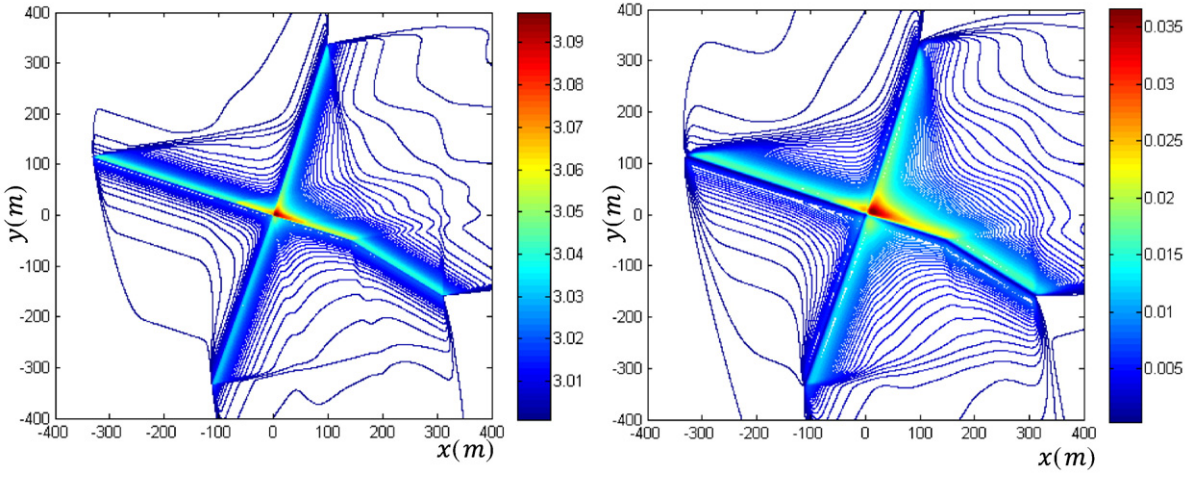

Fig. 9. Average concentration maps in ppm; CO at left; NOx at right, at $z = 2$ m from the ground.

5.5. Pollution evaluation

This instantaneous information of the road traffic permits to reconstruct the instantaneous roads emissions rates calculated for each studied pollutant (Eqs. (14)–(15)), and from the meteorological information and using the Eq. (17), which permits to evaluate the quasi-instantaneous pollution maps respectively for CO and NOx (Figs. 7 and 8). The average pollution maps of the CO and NOx are then obtained from the instantaneous ones (Fig. 9a,b).

The Fig. 7a–d represent instantaneous maps of the CO concentration in the near space of the roundabout. These concentration levels are low according to the WHO maximum exposure levels for carbon monoxide (WHO, 2005). The Fig. 7a shows that the level of pollution remains low until 07: 30 in the morning as the traffic remains moderate and fluid. The maximum CO pollution in this case is 3.14 ppm is obtained at 07 : 50 am. We assume here that the background level of CO is 3 ppm with a contribution of 0.14 ppm due to the road traffic. The lack of experimental information on CO background values in Sousse city compelled us to use an arbitrary 3 ppm value proposed by Lin and Ge (2006). This background value is a constant and it does not affect the logic of the simulations or any pollutant estimation. What is important to notice here is that the contribution of CO from road traffic is very low. In practice, both coupled traffic simulation and experimental measurements are needed to be known in the urban area in order to get an accurate estimation of pollution through the simulated area. The background values are measured experimentally in that case and added to the contribution of the pollution due to the traffic.

During peak periods (around 07 h : 50 am) CO pollution levels remain acceptable (Fig. 7b) and they rise to 3.4 ppm. The peak CO pollution caused by road traffic almost does not affect the air quality of carbon monoxide CO which remains far from reaching the WHO limits (9 ppm for 8 h observation and 35 ppm per hour). For that, the last report of the WHO (2005) does not stress the problem of the carbon monoxide pollution which becomes less topical in the last years, especially with the evolution in catalytic technologies and new engine combustion processes (Sher, 1998).

The NOx essentially results from the reaction of the nitrogen gas present in the air in the combustion chamber of the vehicle in the presence of high temperature. Although catalytic converters and EGR recycling systems can significantly reduce CO, NOx, HC and other gases released from vehicle exhaust, NOx remain one of some difficult pollutants to be completely eliminated at the car exhaust due to certain mechanisms linked to their chemical kinetics of reduction or to the desorption of the catalytic converters (IMechE, 2013). For this purpose, these gaseous pollutants are included among the list of pollutants reported by WHO (2005). The calculations presented in our case study show that the concentration of NOx in the vicinity of the roundabout reaches an instantaneous peak of the order of 0.14 ppm in the morning peak period with a mean on 06 h of 0.035 ppm. We remember that the WHO exposure standards are of 0.12 ppm (40 $\mu g/m^3$) for hourly exposure and 0.106 ppm (200 $\mu g/m^3$) for a mean annual exposure. If the wind speed drops to 0.5 m/s, these standards may be exceeded.

In practice, planners use average pollution maps such as those shown in Fig. 9a for the CO and Fig. 9b for NOx (six hours' concentrations average). The main remark is that a division by two of the wind speed would necessarily double the level of pollution in the area studied. With the CO and NOx averages given in the following figures, it can be stated that the CO may be neglected from future studies of pollution, unlike the hourly NOx which remains close and may even exceed WHO (2005) standards.

In the present work, concentrations levels in the figures (Figs. 7, 8 and 9) are estimated using a Gaussian model. In a Gaussian model, the real geometry of the buildings is not considered, and we assume a global roughness for the studied terrain (Benson, 1989; Zannetti, 1990). This global roughness is added to the Gaussian model, according to the nature of the terrain (Benson, 1989), and the real geometry of the buildings is not no more considered. The contours represented in the figures (Figs. 7, 8 and 9) are only for illustration purposes. A good practice consists in adding a mask in the buildings positions to avoid any misunderstanding of theses contourlines.

6. Conclusion and future work

In this work, we present the steps for the modeling and the implementation of a first order macroscopic road traffic simulation tool, coupled with a pollution dispersion estimation.

The traffic simulation tool permits, from a dynamic origin-destination matrix to quantify the traffic on an urban network using a CTM model for roads and a DNTM for the intersections. Each partial traffic flow $e_{ij}(t)$ starting from an origin i to a destination j is treated as a partial stream and the conservation equations are considered for each of these partial streams. In the case of "20 March" roundabout in Sousse, we simulated road traffic for all 16 partial flows previously measured. After estimating the traffic along the intersection roads, the vehicular emission rates are obtained using the simplified COPERT4 method (CETU, 2012) from a vehicular sample of 1000 vehicles on the city of Sousse. hence, we were able to quantify the hourly and instantaneous maps for Carbon Monoxide CO and NOx Nitrogen Oxides. We notice here that the estimation of pollution from only local directional flow rates observations is not precise because of the heterogeneity of the traffic along the roads (Lin and Ge, 2006). For this, we reproduce the road traffic over the entire road network studied through a simulation in order to guarantee reliable results (Rehimi and Landolsi, 2013). It is worth noting that experimental measurement from at least one monitoring station is needed for the improvement of the simulation results and model.

The numerical results are satisfactory and they represent the first phase for the simulation of the road traffic and the pollution maps estimation throughout the city center of Sousse. It is also a step in the development of low cost solutions in transportation and environment for developing South-Mediterranean countries.

References

Ahn, K., Rakha, H., Trani, A., Van Aerde, M., 2002. Estimating vehicle fuel consumption and emissions based on instantaneous speed and acceleration levels. J. Transp. Eng. 128 (2), 182–190.

Barceló, J., 2010. Fundamentals of Traffic Simulation. Springer Science & Business Media 978-1-4419-6142-6.

Benson, P., 1989. CALINE-4 F A Dispersion Model for Predicting Air Pollutant Concentrations Near Roadways. California Department of Transportation, Sacremeto.

Berkowicz, R., 2000. OSPM - A Parameterised Street Pollution Model; Environmental Monitoring and Assessment. Vol. 65 pp. 323–331.

CALPUFF, 2000. Dispersion Model (Ver. 5) E A User's Guide. Earth Tech Inc., Concord, MA, USA.

Cappiello, A., Chabini, I., Nam, E.K., Lue, A., Abouzeid, M., 2002. A Statistical Model of Vehicle Emissions and Fuel Consumption. In Proceedings the IEEE 5th International Conference Intelligent Transportation Systems, 2002 pp. 801–809 (Singapore).

Casper, J.K., 2010. Fossil Fuelsand Pollution: The Future of Air Quality. Facts On File, Inc. 978-1-4381-2741-5.

CETU, 2012. 'Calcul des Emissions de Polluants des Véhicules Automobiles en Tunnel'. Ministère de l'Écologie du Développement Durable et de l'Énergie. http://www.cetu.developpement-durable.gouv.fr/IMG/pdf/CETU_DocInfo_Calcul_des_Emissions_2012.pdf Last access, 23.07.2016.

Chevallier, E., Leclercq, L., 2007. A macroscopic theory for unsignalized intersections. Transp. Res. B 41, 1139–1150.

Connan, O., Laguionie, P., Maro, D., Hébert, D., Mestayer, P.G., Rodriguez, F., Rodrigues, V., Rosant, J.M., 2015. Vertical and horizontal concentration profiles from a tracer experiment in a heterogeneous urban area. Atmos. Res. 126–137.

Daganzo, C.F., 1994. The cell transmission model: a dynamic representation of highway traffic consistent with the hydrodynamic theory. Transp. Res. B 28, 269–287.

Daiheng, Ni, 2016. Traffic Flow Theory: Characteristics, Experimental Methods, and Numerical Techniques; eBook ISBN: 9780128041475. Elsevier.

Demir, E., Bektas, T., Laporte, G., 2014. A review of recent research on green road freight transportation. Eur. J. Oper. Res. 775–793.

Deng, Q., Lu, C., Yu, Y., Li, Y., Sundell, J., Norback, D., 2016. Early life exposure to traffic-related air pollution and allergic rhinitisin preschool children. Respir. Med. 67-73.

Du, L., Dao, H., 2015. Information dissemination delay in vehicle-to-vehicle communication networks in a traffic stream. IEEE Trans. Intell. Transp. Syst. 16 (1), 66–80.

Du, L., Gong, S., Wang, L., Li, X.Y., 2016. Information-traffic coupled cell transmission model for information spreading dynamics over vehicular ad hoc network on road segments. Transp. Res. C 73, 30–48.

Elliott, J.A., 2013. An Introduction to Sustainable Development. Fourth edition. Taylor and Francis Group, Routledge 978-0-203-84417-5.

EPA, 2003. User's Guide to MOBILE6.1 and MOBILE6.2: Mobile Source Emission Factor Model. Technical Report. United States Environmental Protection Agency, USA http://www.epa.gov/oms/models/mobile6/420r03010.pdf Last access, 01.27.17.

ESDHS, 1997. European Sustainable Development and Health Series: Original English; EUR/ICP/POLC 06 03 05B; City Planning for Health and Sustainable Development.

Godunov, S.K., 1959. A difference scheme for numerical solution of discontinuous solution of hydrodynamic equations. MatematicheskiiSbornik 47, 271–306.

Hausberger, S., Rexeis, M., Zallinger, M., Luz, R., 2009. Emission Factors from the Model PHEM for the HBEFA Version 3. Report Nr. I-20/2009 Haus-Em 33 (08), 679.

HCM, TRB, 2010. Highway Capacity Manual. Transportation Research Board, National Research Council, Washington, DC, USA.

Hossein Shahbazi, H., Taghvaee, S., Hosseini, V., Afshin, H., 2016. A GIS based emission inventory development for Tehran. Urban Climate. 216–229.

IMechE, 2013. Internal Combustion Engines: Performance, Fuel Economy and Emissions. Woodhead Publishing Limited, 2013.

Kouridis, C., Gkatzoflias, D., Kioutsioukis, I., Ntziachristos, L., Pastorello, C., Dilara, P., 2010. Uncertainty Estimates and Guidance for Road Transport Emission Calculations. Technical Report. European Commission Joint Research Centre Institute for Environment and Sustainability http://publications.jrc.ec.europa.eu/repository/handle/111111111/14202 Last access, 01.27.13.

Lebacque, J.P., 2003. Two-phase bounded-acceleration traffic flow model: analytical solutions and applications. Transportation Research Record: Journal of the Transportation Research Board 1852, 220–230.

Lebacque, J.P., 2005. In: Hoogendoorn, S., Bovy, P.H.L. (Eds.), Intersection Modeling, Application to Macroscopic Network Traffic Flow Modeling and Traffic Management.
Lebacque, J.P., Khoshyaran, M., 2005. Transportation and Traffic Theory, Flow, Dynamics and Human Interaction.
Leclercq, L., 2002. Modélisation Dynamique du Trafic et Applications à L'estimation du Bruit Routier. Doctoral Dissertation in Civil Engineering. National Institute of Applied Science, Lyon, France.
Lin, J., Ge, Y.E., 2006. Impacts of traffic heterogeneity on roadside air pollution concentration. Transp. Res. Part D: Transp. Environ. 11 (2), 166–170.
Lipfert, F.W., 2016. A critical review of the ESCAPE project for estimating long-term health effects of air pollution. Environ. Int. (xxx, In Press, Corrected Proof, pp, xxx–xxx).
Ortúzar, J.D., Willumsen, L.G., 2011. Modelling Transport, 4th Edition. Wiley 978-0-470-76039-0.
Pasquill, F., Smith, F.B., 1983. Atmospheric Diffusion: Study of the Dispersion of Windborne Material From Industrial and Other Sources. Third ed. Ellis Horwood, Chichester.
Rehimi, F., Landolsi, J., 2013. The impact of traffic dynamic and wind angle on vehicular emission dispersion. Transp. Res. Part D: Transp. Environ. 21, 1–6.
Sher, E., 1998. Handbook of Air Pollution From Internal Combustion Engines: Pollutant Formation and Control. Academic Press Limited 0-12-639855-0.
Shorshani, M.F., Seigneurm, C., Rehn, L.P., Chanut, H., Pellan, Y., Jaffrezo, J.L., Charron, A., André, M., 2015. Atmospheric dispersion modeling near a roadway under calm meteorological conditions. Transp. Res. D 34, 137–154.
Soulhac, L., Salizzoni, P., Cierco, F.X., Perkins, R., 2011. The model SIRANE for atmospheric urban pollutant dispersion; part I, presentation of the model. Atmos. Environ. 45 (39), 7379–7395.
Tampère, C.M.J., Corthout, R., Cattrysse, D., Immers, L.H., 2011. A generic class of first order node models for dynamic macroscopic simulation of traffic flows. Transp. Res. B 45, 289–309.
Treiber, M., Kesting, A., 2013. Traffic Flow Dynamics: Data, Models and Simulation. Springer.
Venkatram, A., Horst, T.W., 2006. Approximating dispersion from a finite line source. Atmos. Environ. 40 (13), 2401–2408.
WHO, 2005. Air Quality Guidelines. Global Update 2005. Particulate Matter, Ozone, Nitrogen Dioxide and Sulfur Dioxide. World Health Organization (ISBN 92 890 2192 6).
WHO, 2016. Mortality and Burden of Disease From Ambient Air Pollution. http://www.who.int/gho/phe/outdoor_air_pollution/burden/en/# Last access, 24/08/2016.
Zannetti, P., 1990. Air Pollution Modeling: Theories, Computational Methods and Available Software. Springer Science & Business Media.